

Supplementary Information: Photopolymerized Microdomains in both Lipid Leaflets Establish Diffusive Transport Pathways across Biomimetic Membranes

Michelle M. Makhoul-Mansour^a, Joyce B. El-Beyrouthy^a, Hope L. Mumme^b, Eric C. Freeman^a

^a School of Environmental, Civil, Agricultural and Mechanical Engineering, University of Georgia, Athens, Georgia 30602, United States

^b Wallace H. Coulter Department of Biomedical Engineering, Georgia Institute of Technology, Atlanta, Georgia 30332, United States

Materials

Background Buffer Solutions

An aqueous buffer solution was prepared by adding 250 mM Potassium Chloride (KCl, Sigma-Aldrich, St. Louis, MO) and 10 mM 3-(N-morpholino) propanesulfonic acid (MOPS, Sigma-Aldrich, St. Louis, MO) resulting in a pH of ~7.0 as measured. This solution was used when preparing liposomes.

Alpha-Hemolysin Solutions

A concentration of 1.25 µg/mL of wild-type alpha hemolysin (α HL) from *Staphylococcus aureus* (Sigma-Aldrich, St. Louis, MO) was added to the buffer solution and stored at 2 °C.

Gramicidin Solutions

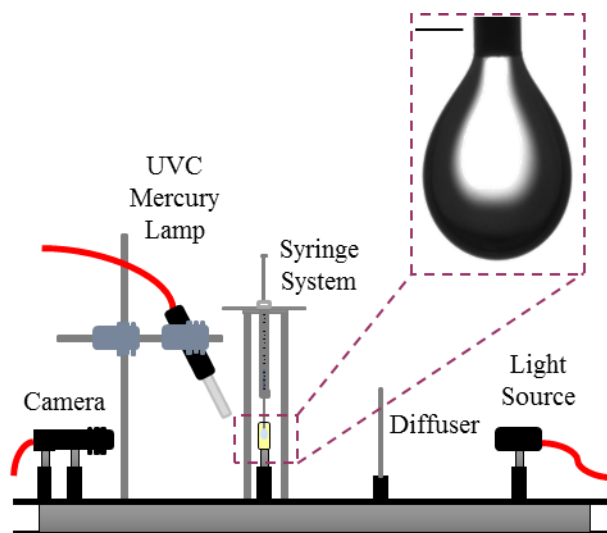
The lipid-in method for DIB formation is used in this case, where lipids are dissolved in the aqueous phase. Zwitterionic lipids (1,2-diphytanoyl-sn-glycero-3-phosphocholine (DPhPC), Avanti Polar Lipids, Alabaster, AL) were suspended in the aqueous buffer solution (250 mM KCl and 10 mM MOPS) at a concentration of 2.5 mg/ml. All lipid solutions were sonicated using a probe tip sonicator (QSONICA Q55 Probe Tip Ultrasonicator, QSONICA, Newtown, CT) and afterwards stored at 2 °C. Gramicidin from *Bacillus aneurinolyticus* (*Bacillus brevis*, Sigma-Aldrich, St. Louis, MO) a linear polypeptide antibiotic complex is tested in this work. A mixture of *gramicidin A, B, C, and D* was first dissolved at a concentration of 50 mg/ml in methanol (Sigma-Aldrich, St. Louis, MO). This solution was further diluted to a concentration of 5 mg/ml. Following an additional 2000-fold dilution, gramicidin was added to the above lipid-water solution at a concentration of 25 ng/ml. All solutions containing gramicidin were kept in the dark and stored at 2 °C.

DiynePC Solutions

A mixture of 1,2-di- (10z,12z-tricosadiynoyl)-sn-glycero-3-phosphocholine (23:2 DiynePC, Avanti Polar Lipids, Alabaster, AL)) polymerizable lipids and zwitterionic lipids (DPhPC) at 1:8, 1:4, 1:2, and 0:1 (control case, contains only DPhPC) mass ratios respectively were first dissolved in chloroform (Sigma-Aldrich, St. Louis, MO) to assure a homogenous mixture yielding clear solutions in the organic solvent. Once lipid combinations were thoroughly mixed in the organic solvent, chloroform was then removed through evaporation using a dry argon stream in a fume hood. The resulting lipid film was then further dried to remove residual traces of chloroform by placing the vial in a vacuum chamber for a minimum of 6 hours. Lipid film hydration was accomplished by adding an aqueous buffer solution (250 mM KCl and 10 mM MOPS) to the vials followed by gentle agitation. The final lipid concentration in each solution was 2.5 mg/ml. These solutions subsequently underwent several thaw-freeze cycles (a minimum of 5 cycles) and were afterwards kept in the dark and stored at 2 °C. Upon usage, the solutions were sonicated using a probe tip sonicator (2 mm standard probe tip with a maximum oscillation amplitude of 200 µm, from QSONICA Q55 Probe Tip Ultrasonicator, QSONICA, Newtown, CT) until a clear consistency was achieved and no lipids aggregations were observed. Sonication was held in 30 W cycles of 3 minutes each at a temperature less than the transition temperature of these lipids (≤ 40 °C¹). On average, a minimum of 5 cycles was required before the solutions became clear.

Oil Solutions

Typically, the lipid-in and out methods for DIB formation were simultaneously used². Zwitterionic lipids (DPhPC) were suspended in a 2:1 (volume ratio) mixture of hexadecane and silicone oil AR20 (both Sigma-Aldrich, St. Louis, MO) at a concentration of 0.5 mg/ml. All oil-lipid solutions were sonicated for 20 minutes (Elmasonic S100h Ultrasonic sonicator, Elma Schmid Bauer GmbH, Gottlieb-Daimler-Straße Singen, Germany) and afterwards stored at 2 °C. Each lipid-oil solution was then refreshed by sonicating for 15 minutes prior to each use. This oil mixture was found to increase the bilayers' stability^{3, 4}. When specifically stated,



Supplementary Figure 1. Schematic representation of the pendant drop experimental setup for measuring the interfacial surface tension. The diffused light of a halogen lamp passes through a Quartz cuvette. Once the measurements have been executed, samples of the water-lipid mixtures were set aside and exposed for 5 minutes to UVC light using the UVC Mercury lamp shown in this schematic. Scale bar represents 300 μm .

hexadecane (Sigma Aldrich, St. Louis, MO) was used as the surrounding continuous phase with no further modifications in order to isolate the effect of photopolymerizable lipids. Please note that no polymerizable lipids were dissolved in the oil phase but only the zwitterionic non-polymerizable phospholipids (DPhPC), ensuring control over the DiynePC distribution within the membrane.

Calcein Solutions

Mixtures of 23:2 DiynePC polymerizable lipids (also referred to as C23 lipids) and Zwitterionic lipids (DPhPC) at 1:4 and 0:1 (control case, contains only DPhPC) mass ratios were suspended in an aqueous buffer solution (250 mM KCl and 10 mM MOPS) at a concentration of 0.25 mg/mL. Calcein (Cayman Chemical Company, Ann Arbor, MI) was added to the solutions at a 0.25 mg/mL concentration. Calcein has an excitation wavelength of 495 nm, an emission wavelength of 515 nm and a net charge of -3. These solutions were exposed to UV-C light (as described in this document) for 5 minutes prior to the addition of calcein.

Experimental Methods

UV-C Induced Polymerization

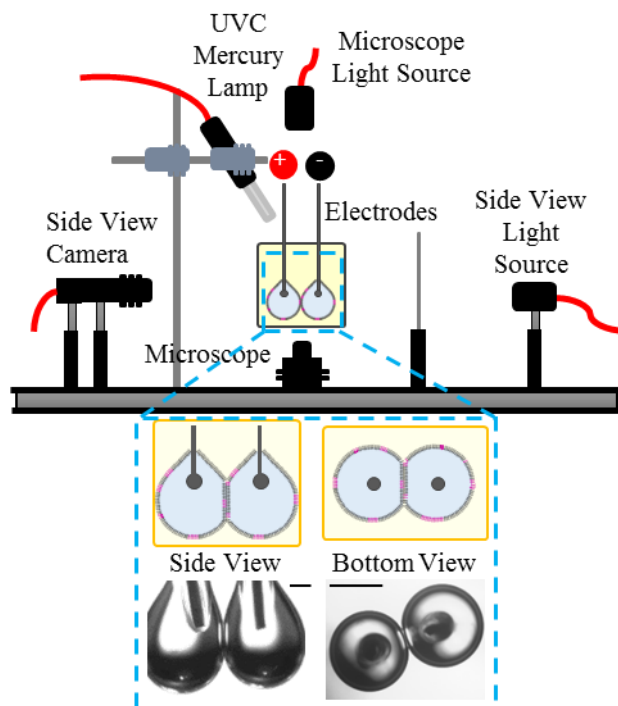
A UV-C mercury lamp (11.73 cm total length, 254 nm supplied wavelength, Analytik Jena, Jena, Germany) connected to an input power supply (PS-1 AC Power Supply, 115 V/60 Hz, Analytik Jena, Jena, Germany) was placed 5-7 cm away from the lipid solutions vials for 5 minutes (polymerization occurring rapidly for different diacetylene infused lipids at short irradiation times and decreasing in rate for periods longer than that⁵). After UV-C exposure, the previously transparent lipid solutions would assume their pre-sonication white-opaque colour indicating that polymerization had occurred. Lipid polymerization was also performed after droplet deposition on site in a similar manner.

Protocol for Electrophysiological Measurements

The obtained current traces were recorded in voltage-clamp mode (Whole Cell $\beta = 1$) at a sampling frequency of 10 kHz and filtered at 1 kHz using the embedded low-pass Bessel filter (-80 dB/decade). Post-acquisition, a 500 Hz fourth-order Butterworth low-pass filter was applied in MATLAB before plotting the measured current traces. All measurements were carried in a dark room to minimize the possibility of spontaneous lipid crosslinking (although very minimal⁶) and reduce external noise. This approach was used for all electrical recordings unless specifically stated otherwise.

Alpha-Hemolysin/Gramicidin Functionality

The obtained current traces with a DC applied voltage of +50 mV were recorded using the previously described electrophysiological protocol. Changes in the current reflect changes in the membrane conductance, either through the insertion of pores or generation of defects in the membrane structure.



Supplementary Figure 2. Schematic representation of the bilayer characterization experimental setup. Side and bottom view images of the lipid bilayer are simultaneously acquired using two different cameras. These images are then used to determine the bilayer's dimensions and by extension its area. Properties of the bilayers are evaluated pre and post UV-C exposure and lipid polymerization. Droplets are suspended from Ag/AgCl electrodes. Scale bars represent 250 μm each.

Single Bilayer Conductivity with DiynePC

Using the same experimental setup for assessing bilayer properties (described in detail in the following section), the change in bilayer electrical conductivity upon the gradual introduction of polymerizable lipids was analysed for the hexadecane: silicone oil AR20 lipid-mixture as well as for bilayers formed in hexadecane oil. Four different sub-cases were analysed: a classical control subcase with no polymerizable lipids and three additional subcases where the polymerizable lipids were introduced at ratios of 1:8, 1:4 and 1:2 DiynePC:DPhPC by mass. In all cases, the conductivity of every bilayer was examined prior to any UV-C exposure. The droplets were then separated and exposed for 5 minutes to UV-C-light as previously described. Following their exposure and the formation of cross-linked rafts in the lipid monolayers, the droplets were brought into contact to form the membrane and the conductivity of the bilayer was assessed again. Current traces obtained for various applied voltages ranging from +50 to +150 mV were recorded using the previously described electrophysiological protocol. It is possible to photopolymerize the DIB membrane directly when droplets are in contact and even separate droplets, expose them to UV-C light and the reform the lipid bilayer. However direct UV-C exposure produces significant noise in our measurements (also noted by previous works⁷) so all electrical equipment had to be disconnected during UV-C exposure. Cases where either bilayer were polymerized in situ while the droplets were still in contact, or cases where droplets were separated, exposed to UV-C light and the bilayers reformed were similarly conducted but current traces could not be recorded due to the high level of noise produced by the UV-C lamp.

Measurements of Interfacial Properties

Measurement of Monolayer Interfacial Tensions

Surface tensions of lipid monolayers were assessed using the pendant drop technique and open source software OpenDrop⁸ as described in previous works^{9,10} and depicted in **Supplementary Figure 1**. Interfacial tension was assessed for four different lipid mixtures with a 2:1 hexadecane:silicone oil AR20 mixture containing 0.5 mg/mL DPhPC as the continuous phase. The tested aqueous phases include a control case with no polymerizable lipids (only DPhPC was included), then cases with 1:8, 1:4, and 1:2 DiynePC:DPhPC (**Table 1**). The same measurements were repeated in hexadecane oil alone without dissolved lipids (**Table 2**).

Measurements of DIB Specific Capacitance, Angle of Contact, Bilayer Tension, Adhesion Energy and Thickness

A DIB may be electrically approximated as a capacitor in parallel with a high amplitude resistance^{11,12}. Since the membrane resistance is often in the order of $G\Omega$ - $T\Omega$ ^{11,13}, the resistive current is mostly negligible, and the overall current of a bilayer reduced

to its capacitive component. However, in cases where a porous bilayer is anticipated, this resistive current is no longer negligible and constitutes a part of the current response. An evaluation of photopolymerizable DIBs specific capacitance, thickness, bilayer tension, angle of contact (defined herein as being the total angle between the droplets at equilibrium), energy of adhesion and specific conductance (defined as the ratio of the average cross-bilayer current with a constant +100 mV measured for 10 minutes divided by the bilayer area) is conducted using *in situ* DIB characterization techniques frequently used and tested^{3, 10, 14-16}. Since some resistive current is anticipated, a 10 mV, 50 Hz sine wave voltage was applied (33120A function generator, Hewlett-Packard, Palo Alto, CA) when evaluating the nominal capacitance of the bilayers. A MATLAB script is used to extract the capacitive and resistive components of the measured current through curve-fitting. Droplets (~500 μm radius) were systematically injected on agarose (2% by mass EZ Pack Agarose LE, Molecular Biology Grade, Benchmark Scientific, Sayresville, NJ) coated silver/silver chloride (Ag/AgCl) electrodes (125 μm in diameter, GoodFellow, Coraopolis, PA). Each electrode position was controlled through a three-axis manual micromanipulator (Siskiyou, Grants Pass, OR). All electrical measurements were acquired using previously described electrophysiological protocol and conducted using the AXOpatch 200B patch clamp amplifier and the Digidata 1440A data acquisition system (Molecular Devices, Sunnyvale, CA). Stray capacitance was accounted before beginning any measurement by using the patch-clamp amplifier built-in whole-cell compensation. When evaluating each case, bottom-view images of the pre-formed, stabilized DIB were acquired using a CCD camera (high sensitivity DCC1645C-HQ, Thorlabs, Newton, NJ) mounted on an inverted microscope. Cross-sectional images of the droplets were also acquired using a CCD camera (high sensitivity DCC1240C, Thorlabs, Newton, NJ) to which zoom lenses (6.5X zoom lenses with a 0.7–4.5 \times magnification range, Thorlabs, Newton, NJ) were attached. **Supplementary Figure 2** shows a schematic representation of this experimental setup. A more accurate determination of the lipid-bilayer area can be obtained by approximating the contact of the two droplets with an ellipse whose major and minor axes are those obtained from the cross-sectional images¹⁶. Bilayer properties in hexadecane as well as the 2:1 hexadecane:silicone oil AR20 DPhPC mixture were assessed for four different cases: a control case with no polymerizable lipids (only DPhPC was included), and cases with 1:8, 1:4, and 1:2 DiynePC:DPhPC mass ratios. For each case, 7 samples were evaluated and the corresponding data (average and standard deviation) reported. A linear 4 mV/s voltage-sweep for these bilayers was also performed and current responses recorded.

Bilayer Network Directional Conductivity upon DiynePC Introduction

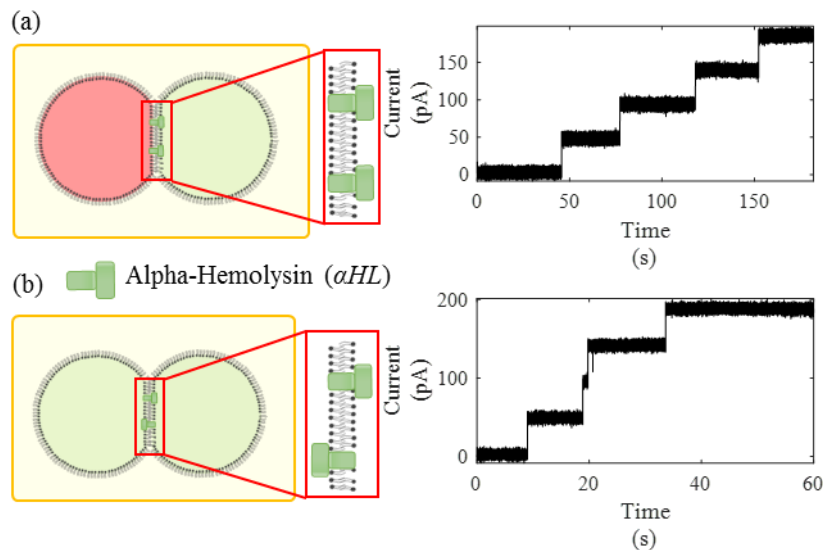
Droplets (~400 μm radius, the size of these droplets was mainly restricted by the size of the in-house made crate substrate) were systematically injected first on agarose coated silver/silver chloride electrodes. These two droplets are referred to as input droplets. Additional droplets were deposited in the same fashion into the wells of a crate substrate from previous studies¹⁷. The droplets were placed in their initial positions using a glass rod (GR100-4 Glass Rod, World Precision Instruments, Inc., Sarasota, FL) pulled to fine points using a programmable pipet puller with pretested settings. All electrical measurements were acquired using the previously described electrophysiological protocol. The total voltage applied on the networks was varied so that each bilayer had an individual applied voltage of +100 mV and was estimated using a bilayer-equivalent circuit model⁴. Images were acquired using a CCD camera (DCC1645C-HQ, Leica Microsystems, Wetzlar, Germany) mounted on an inverted fluorescent microscope (Leica DMI3000B manual inverted microscope, Leica Microsystems, Buffalo Grove, IL). The 2:1 hexadecane:silicone oil AR20 lipid-oil mixture mentioned in previous sections was used. Two types of lipid-aqueous solutions were used: a first polymerizable type (marked in blue in various figures) and a second non-polymerizable type (marked otherwise in red). The first type consists of the aqueous lipid suspension with a 1:4 DiynePC: DPhPC ratio of lipids mentioned in a previous section. This solution was treated with UV-C light for 5 minutes prior to each experiment. The second solution contained DPhPC alone.

Calcein Diffusion Across a Single Lipid Bilayer

Calcein was always introduced from the reference side of the bilayer only (donor droplet). Two cases were studied for 120 minutes each. In the first case (control case) the donor droplet contained pre-polymerized 23:2 DiynePC and DPhPC (at a mass ratio of 1:4). Meanwhile, the acceptor droplet contained only non-polymerizable DPhPC phospholipid. In the second case, both droplets contained pre-polymerized 23:2 DiynePC (at a 1:4 mass ratio with DPhPC). A -100 mV constant voltage was applied in all cases and the hexadecane silicone oil AR20 DPhPC oil-lipid mixture was used as an external phase. Fluorescent microscopy (Leica DMI3000B inverted microscope with a connected External light source for fluorescence excitation Leica EL6000, Leica Microsystems, Buffalo Grove, IL) was used to visualize calcein. Images were acquired every 5 minutes and used to determine the diffusion of calcein across lipid bilayers. ImageJ software (NIH) was used to quantify the fluorescent intensity of both donor and acceptor droplets with time. The fluorescent intensity was measured along the line passing by the centre of the droplet and perpendicular to the line intersecting the DIB: intensity was then averaged from the edge of the DIB to a distance of 125 μm across this line. The relative intensity is then the ratio of the average intensity in the acceptor droplet to that in the donor droplet.

Supplementary Results

α HL Insertion Activity in a Single Lipid Bilayer

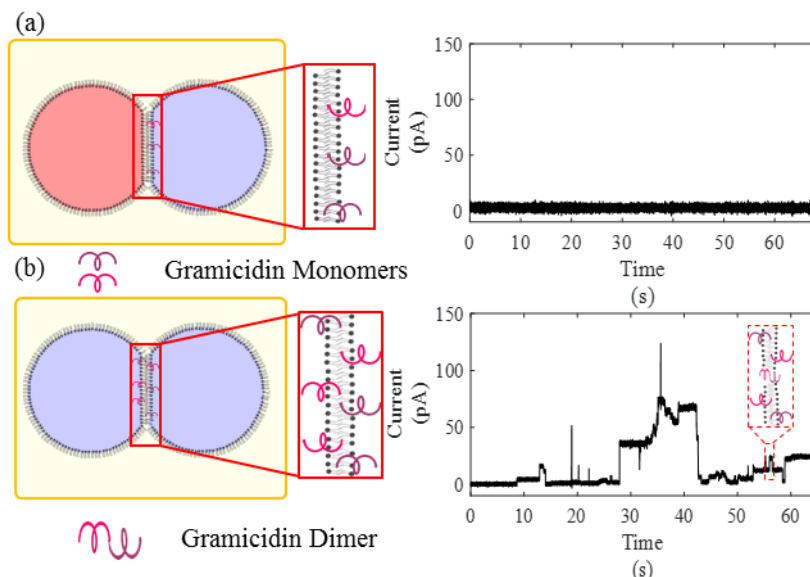


Supplementary Figure 3. α HL insertion activity is showcased upon the application of a constant +50 mV voltage as a typical current response with stepwise increases. In all cases, α HL was added at a concentration of 1.25 μ g/mL. (a) shows the current response whenever α HL was added to the reference side of the bilayer. Meanwhile (b) shows the current response when α HL was added to both sides of the bilayer. All measurements were recorded in voltage clamp mode at a sampling frequency of 10 kHz and filtered at 1 kHz (using the embedded low-pass Bessel filter -80 dB/decade). Post-acquisition, data was filtered at 500 Hz using a fourth order Butterworth low-pass filter in MATLAB.

The α HL insertion mechanism is spontaneous^{18, 19}. This PFT inserts into a lipid bilayer by oligomerizing cooperatively into hexamers or heptamers on the membrane surface¹⁸. These heptamers then insert into lipid bilayers to form mushroom-shaped pores that allow passage of small molecules²⁰. While showing different sensitivity depending on membrane composition, the full insertion mechanism of α HL happens whether the monomers are present on one or both sides of the bilayer^{18, 20-22}. As shown from the current traces with a fixed +50 mV potential in **Supplementary Figure 3**, α HL retained its activity whether it was added asymmetrically from one side of the bilayer (trans side as shown in **Supplementary Figure 3.a.**) or symmetrically from both sides of the bilayer (cis and trans sides as shown in **Supplementary Figure 3.b.**). Each additional α HL insertion event was marked by the stepwise increase in the measured current. The insertion of α HL does not show any significant differences between having the initiating monomers present on one side or both sides of the bilayer as shown here and can by extension occur between a droplet containing the pore forming toxin (PFT) and any other droplet, generating additional channels which might cause undesired changes in the qualities of adjacent membranes.

Gramicidin Insertion Activity in a Single Lipid Bilayer

Gramicidin channels are cross-membrane structures. When dissolved, gramicidin structures exist as mixtures of parallel and antiparallel dimers as well as disordered monomers²³⁻²⁵. Gramicidin channels across the membrane are formed from the dimerization of helical monomers that had been inserted into each monolayer leaflet. These channels can be either (i) symmetrical dimers with a single conductance state, or (ii) homodimers with different conductance states or even (iii) heterodimers formed between dissimilar homologues with multiple conductance states²⁶. In all cases, the monomers have to be present on both sides of the DIB for insertion to occur – changes in the conductivity are not exhibited with the asymmetric introduction of gramicidin. This property of the dimers was confirmed within the DIB platform in **Supplementary Figure 4**, as the current trace in panel a indicates no dimerization in the bilayer while that of panel b clearly shows different dimerization incidences with different conductance levels as expected from the employed gramicidin mixtures when the membrane potential is held constant at 50 mV. This limits the droplet-droplet exchange to droplet pairs that both contain gramicidin. Yet the concern with using gramicidin in DIB structures lies in its selectivity²⁶⁻²⁸. These gramicidin dimeric pores exhibit a selectivity for small monovalent cations²⁸⁻³⁰ posing additional challenges for the transport of anionic or larger molecules.



Supplementary Figure 4. The typical response of +50 mV constant voltage applied to bilayers for Gramicidin are brief current stepwise discrete increments, resulting from the transient dimerization of the peptide. A mixture of Gramicidin A, B, C and D were used at a concentration of 25 ng/ml resulting in response current steps with different amplitudes. Gramicidin was added from the reference side only in (a) compared to both sides in (b). All measurements were recorded in voltage clamp mode at a sampling frequency of 10 kHz and filtered at 1 kHz (using the embedded low-pass Bessel filter -80 dB/decade). Post-acquisition, data was filtered at 500 Hz using a fourth order Butterworth low-pass filter in MATLAB.

Interfacial Properties of DIBs

The key results are summarized in the main text, **Figure 7**. The measured parameters for the 2:1 hexadecane:silicone oil AR20 with 0.5 mg/mL DPhPC and hexadecane solvents are listed here in **Supplementary Table 1** and **Supplementary Table 2**. The energy of adhesion reflects the favorability of membrane formation, and is defined by the difference in energy per area replacing two monolayer surfaces with a single bilayer, or $2\gamma_m - \gamma_b$. The bilayer thickness is calculated by approximating the membrane as a parallel plate capacitor, where $h = \epsilon_0 \epsilon_r / C_s$. h is the bilayer dielectric thickness, ϵ_0 is vacuum permittivity, ϵ_r is the relative permittivity of the membrane interior (2.2^{3,10}), and C_s is the specific capacitance of the membrane.

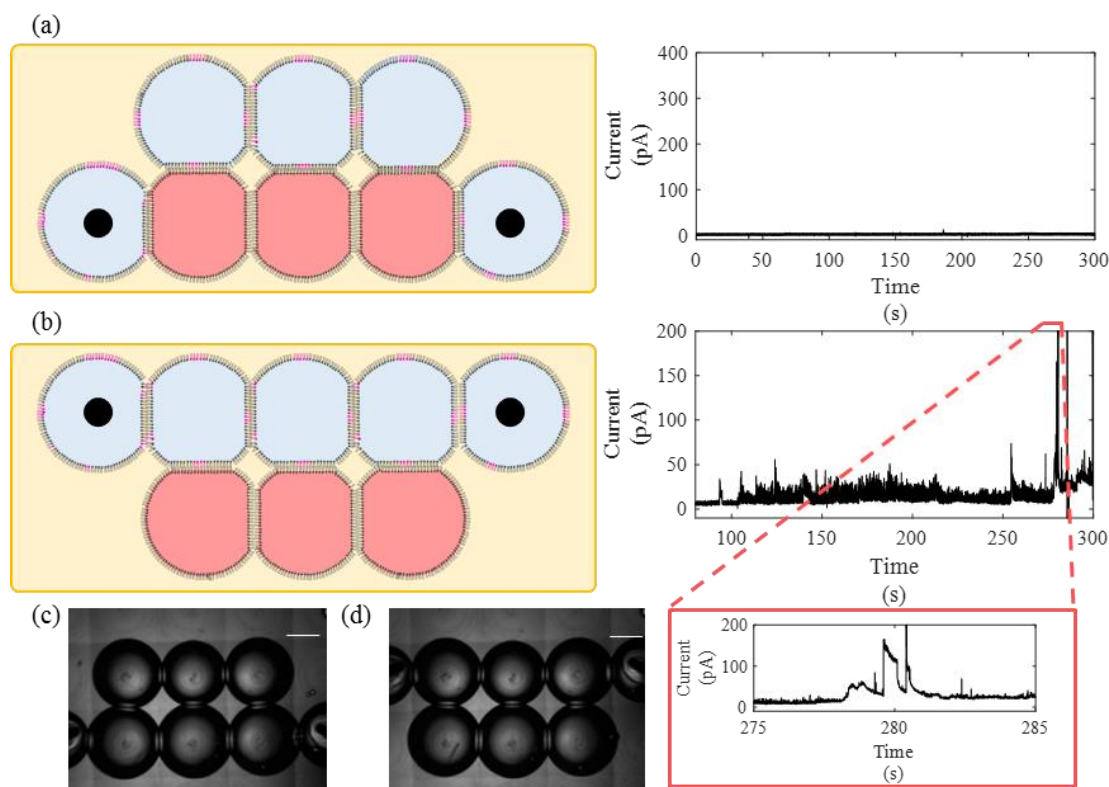
Supplementary Table 1. Measurement of the properties of DIBs in 2:1 hexadecane:silicone 0.5 mg/mL DPhPC lipid-oil mixture with different ratios of polymerizable lipids dissolved in the aqueous phase (2.5 mg/ml total) before and after 5 minutes UV-C exposure. Each experiment was repeated 7 times. The standard deviation is reported for directly measured values including the monolayer tension and angle of contact. Errors in the remaining secondary values are calculated using error propagation.

DiynePC	DPhPC	monolayer tension (mN/m)	angle of contact (deg)	specific capacitance ($\mu\text{F}/\text{cm}^2$)	energy of adhesion (mN/m)	bilayer tension (mN/m)	bilayer thickness (\AA)	specific conductance ($\times 10^{-2} \mu\text{S}/\text{cm}^2$)
1	2	1.04 (± 0.05)	39.60 (± 0.38)	0.67 (± 0.01)	0.12 (± 0.10)	1.95 (± 0.01)	29.14 (± 0.34)	0.04 (± 0.002)
1	4	0.98 (± 0.08)	37.17 (± 3.21)	0.65 (± 0.05)	0.10 (± 0.10)	1.85 (± 0.05)	30.34 (± 2.50)	0.24 (± 0.15)
1	8	1.06 (± 0.04)	42.77 (± 2.56)	0.70 (± 0.06)	0.16 (± 0.08)	1.98 (± 0.02)	28.04 (± 2.21)	0.25 (± 0.02)
0	1	0.97 (± 0.02)	48.20 (± 2.35)	0.72 (± 0.02)	0.17 (± 0.04)	1.76 (± 0.01)	27.26 (± 0.81)	0.06 (± 0.01)
UVC (254 nm wavelength) applied to drop phase for 5 minutes								
1	2	1.18 (± 0.02)	40.61 (± 0.65)	0.65 (± 0.03)	0.15 (± 0.04)	2.22 (± 0.01)	30.41 (± 1.64)	463.79 (± 309.06)
1	4	0.96 (± 0.06)	33.16 (± 2.36)	0.75 (± 0.04)	0.08 (± 0.07)	1.86 (± 0.03)	26.01 (± 1.34)	451.00 (± 108.09)
1	8	1.10 (± 0.22)	44.30 (± 1.90)	0.70 (± 0.06)	0.16 (± 0.14)	2.03 (± 0.16)	28.24 (± 2.13)	65.07 (± 30.67)
0	1	1.03 (± 0.01)	51.95 (± 1.74)	0.68 (± 0.01)	0.21 (± 0.02)	1.85 (± 0.01)	28.54 (± 0.49)	0.06 (± 0.02)

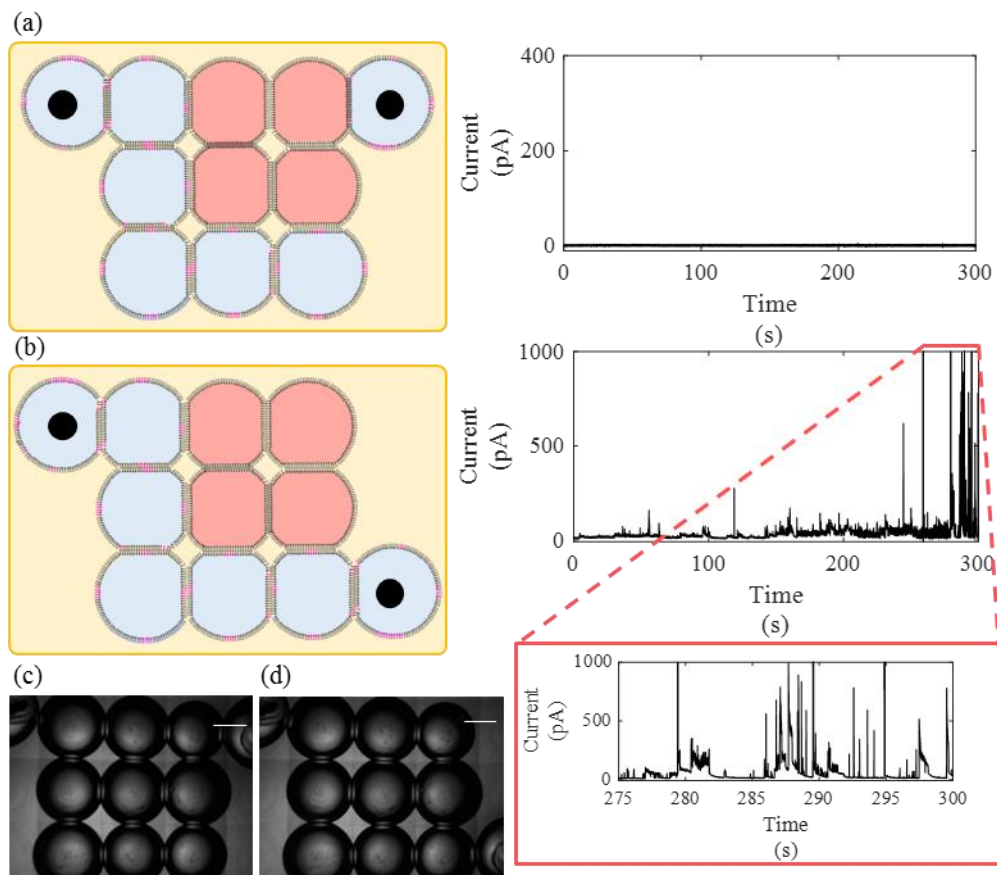
Supplementary Table 2. Measurement of the properties of DIBs in hexadecane (no dissolved lipids) with different ratios of polymerizable lipids dissolved in the aqueous phase (2.5 mg/ml total) before and after 5 minutes UV-C exposure. Each experiment was repeated 7 times. The standard deviation is reported for directly measured values including the monolayer tension and angle of contact. Errors in the remaining secondary values are calculated using error propagation.

DiynePC	DPhPC	monolayer tension (mN/m)	angle of contact (deg)	specific capacitance ($\mu\text{F}/\text{cm}^2$)	energy of adhesion (mN/m)	bilayer tension (mN/m)	bilayer thickness (\AA)	specific conductance ($\times 10^{-2} \mu\text{S}/\text{cm}^2$)
1	2	1.68 (± 0.27)	30.51 (± 3.38)	0.59 (± 0.06)	0.11 (± 0.11)	3.24 (± 0.24)	33.26 (± 3.44)	0.18 (± 0.01)
1	4	1.13 (± 0.07)	34.10 (± 5.03)	0.53 (± 0.05)	0.12 (± 0.10)	2.16 (± 0.11)	36.99 (± 3.18)	0.19 (± 0.02)
1	8	1.15 (± 0.12)	38.49 (± 3.11)	0.61 (± 0.08)	0.13 (± 0.12)	2.21 (± 0.07)	32.23 (± 3.63)	0.25 (± 0.03)
0	1	1.11 (± 0.04)	51.87 (± 6.14)	0.60 (± 0.08)	0.22 (± 0.08)	1.99 (± 0.06)	32.97 (± 5.03)	0.22 (± 0.03)
UVC (254 nm wavelength) applied to drop phase for 5 minutes								
1	2	2.02 (± 0.32)	20.46 (± 3.54)	0.44 (± 0.12)	0.07 (± 0.06)	3.97 (± 0.43)	46.49 (± 10.33)	648.25 (± 145.79)
1	4	1.41 (± 0.57)	31.54 (± 2.25)	0.52 (± 0.03)	0.11 (± 0.07)	2.71 (± 0.91)	37.26 (± 1.74)	449.92 (± 156.22)
1	8	1.04 (± 0.03)	35.85 (± 3.62)	0.56 (± 0.05)	0.10 (± 0.06)	1.98 (± 0.02)	35.04 (± 3.06)	85.06 (± 40.04)
0	1	1.07 (± 0.06)	50.23 (± 0.74)	0.67 (± 0.02)	0.20 (± 0.12)	1.94 (± 0.01)	29.04 (± 0.64)	0.25 (± 0.01)

Pore Formation in Networks



Supplementary Figure 5. Blue droplets contain both polymerizable and non-polymerizable phospholipids (23: 2 DiynePC and DPhPC) dissolved at a concentration of 2.5 mg/ml in a 2:1 hexadecane:silicone oil AR20 0.5 mg/mL DPhPC oil-lipid mixture. Meanwhile, red droplets only contain DPhPC. The ratio of polymerizable to non-polymerizable lipids was a 1:4 by mass. In (a), the micro switch was switched OFF by moving the input droplets so that red droplets are placed between the two. In (b), the micro switch was turned to the ON configuration by moving the input blue droplets connected to the acquisition system so that all droplets containing polymerizable lipids were aligned. Bilayers were then given time to form and the corresponding current recorded. (c) and (d) show the images acquired for (a) and (b) respectively. All measurements were recorded in voltage clamp mode at a sampling frequency of 10 kHz and filtered at 1 kHz (using the embedded low-pass Bessel filter -80 dB/decade). Post-acquisition, data was filtered at 500 Hz using a fourth order Butterworth low-pass filter in MATLAB. Scale bars represent $400 \mu\text{m}$ each.



Supplementary Figure 6. Blue droplets contain both polymerizable and non-polymerizable phospholipids (23: 2 DinynePC and DPhPC) dissolved at a concentration of 2.5 mg/ml in a 2:1 hexadecane:silicone oil AR20 0.5 mg/mL DPhPC oil-lipid mixture. Meanwhile, red droplets only contain DPhPC. The ratio of polymerizable to non-polymerizable lipids was a 1:4 by mass. . In (a), the micro switch was switched OFF by moving the input droplets so that red droplets are placed between the two. In (b), the micro switch was turned to the ON configuration by moving the input blue droplets connected to the acquisition system so that all droplets containing polymerizable lipids were aligned. Bilayers were then given time to form and the corresponding current recorded. (c) and (d) show the images acquired for (a) and (b) respectively. All measurements were recorded in voltage clamp mode at a sampling frequency of 10 kHz and filtered at 1 kHz (using the embedded low-pass Bessel filter -80 dB/decade). Post-acquisition, data was filtered at 500 Hz using a fourth order Butterworth low-pass filter in MATLAB. Scale bars represent $400\ \mu\text{m}$ each.

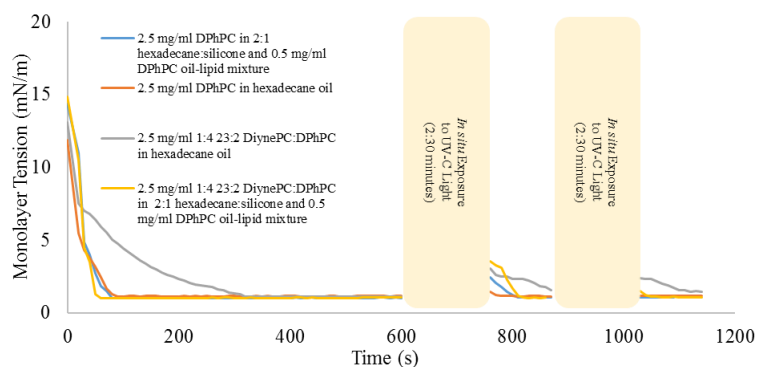
Supplementary Figure 5 and **Supplementary Figure 6** provide additional examples of conductive pathways established by linking chains of droplets containing photopolymerized DinynePC. In each of these cases the conductivity is only increased when each droplet between the two electrodes contains the photoresponsive lipids. These plots are similar to **Figure 9** in the primary text with larger networks of droplets.

Measurement of Monolayer Interfacial Tensions

Supplementary Table 3 contains the measure monolayer surface tension with increasing UV-C exposure with varying lipid ratios and surrounding solvents. The kinetics of monolayer formation are also presented in **Supplementary Figure 7**. All cases show a rapid initial decay in the monolayer tension as lipids assemble at the oil-water interface. The 1:4 DinynePC:DPhPC mixture in hexadecane without lipids in the surrounding solvent is the one exception, noting a greater period of time necessary for liposome unfolding and monolayer assembly. After the monolayers were established as indicated by a stable interfacial tension, image acquisition was paused for UV-C exposure for 150 seconds. After each exposure, the monolayer tension increased temporarily before decaying back to a value that was slightly above the previous equilibrium tension.

Supplementary Table 3. Equilibrium monolayer tension results for different aqueous lipid mixtures exposed directly on-site to UV-C light presented in **Supplementary Figure 7**.

Monolayer Tension average	2.5 mg/ml DPhPC in 2:1 hexadecane:silicone and 0.5 mg/ml DPhPC oil-lipid mixture	2.5 mg/ml DPhPC in hexadecane oil	2.5 mg/ml 1:4 23:2 DiynePC:DPhPC in hexadecane oil	2.5 mg/ml 1:4 23:2 DiynePC:DPhPC in 2:1 hexadecane:silicone and 0.5 mg/ml DPhPC oil-lipid mixture
pre UV-C	1.02	1.15	1.11	1.07
+2:30 mins UV-C	1.06	1.14	1.72	1.04
+2:30 mins UV-C	1.08	1.16	1.45	1.08



Supplementary Figure 7. Monolayer tension results for different aqueous lipid mixtures exposed directly on-site to UV-C light. Aqueous solutions are first introduced into the oil phase and the monolayer tension measured. The droplets are then exposed to UV-C light for 2:30 minutes and the subsequent monolayer tension measured for the following 2 minutes. This process is repeated again and the tension measured. The monolayer tension could not be measured during exposure to UV-C light since the camera had to be covered to prevent any damage to the lenses. In the contrary, the results reported in **Table 1** and **Table 2** in the main manuscript correspond to aqueous solutions that have been pre-exposed to UV-C light for 5 minutes.

Notes and References

1. A. Blume, *Chemistry and physics of lipids*, 1991, **57**, 253-273.
2. W. L. Hwang, M. Chen, B. Cronin, M. A. Holden and H. Bayley, *Journal of the American Chemical Society*, 2008, **130**, 5878-5879.
3. G. J. Taylor, G. A. Venkatesan, C. P. Collier and S. A. Sarles, *Soft Matter*, 2015, **11**, 7592-7605.
4. E. J. Challita, M. M. Makhoul-Mansour and E. C. Freeman, *Biomicrofluidics*, 2018, **12**, 034112.
5. J. Leaver, A. Alonso, A. A. Durrani and D. Chapman, *Biochimica et biophysica acta (BBA)-biomembranes*, 1983, **732**, 210-218.
6. D. S. Johnston, S. Sanghera, M. Pons and D. Chapman, *Biochimica et Biophysica Acta (BBA)-Biomembranes*, 1980, **602**, 57-69.
7. S. Punnamaraju, H. You and A. Steckl, *Langmuir*, 2012, **28**, 7657-7664.
8. J. D. Berry, M. J. Neeson, R. R. Dagastine, D. Y. C. Chanc and R. F. Taborf, *Journal of Colloid and Interface Science*, 2015, **454**, 226-237.
9. G. A. Venkatesan, J. Lee, A. B. Farimani, M. Heiranian, C. P. Collier, N. R. Aluru and S. A. Sarles, *ACS-Langmuir*, 2015, **31**, 12883-12893.
10. M. Makhoul-Mansour, W. Zhao, N. Gay, C. O'Connor, J. Najem, L. Mao and E. C. Freeman, *Langmuir*, 2017.
11. H. Bayley, B. Cronin, A. Heron, M. A. H. W. L. H. R. Syeda, J. Thompson and M. Wallace, *Royal Society of Chemistry* 2008, **4**, 1191-1208.
12. M. A. Holden, D. Needham and H. Bayley, *Journal of the American Chemical Society*, 2007, **129**, 8650-8655.
13. C. Danelon, J.-B. Perez, C. Santschi, J. Brugger and H. Vogel, *Langmuir*, 2006, **22**, 22-25.
14. L. C. Gross, A. J. Heron, S. C. Baca and M. I. Wallace, *Langmuir*, 2011, **27**, 14335-14342.
15. L. C. M. Gross, Doctor of Philosophy, University of Oxford 2011.
16. J. D. Rofeh, University of California Santa Barbara, 2017.

17. E. C. Freeman, A. B. Farimani, N. R. Aluru and M. K. Philen, *Biomicrofluidics*, 2015, **9**, 064101.
18. M. W. Parker and S. C. Feil, *Prog Biophys Mol Biol*, 2005, **88**, 91-142.
19. I. Iacovache, F. G. van der Goot and L. Pernet, *Biochimica et Biophysica Acta (BBA)-Biomembranes*, 2008, **1778**, 1611-1623.
20. L. Song, M. R. Hobaugh, C. Shustak, S. Cheley, H. Bayley and J. E. Gouaux, *Science*, 1996, **274**, 1859-1865.
21. J. E. Gouaux, O. Braha, M. R. Hobaugh, L. Song, S. Cheley, C. Shustak and H. Bayley, *Proceedings of the National Academy of Sciences*, 1994, **91**, 12828-12831.
22. S. E. Henrickson, M. Misakian, B. Robertson and J. J. Kasianowicz, *Phys Rev Lett*, 2000, **85**, 3057-3060.
23. W. R. Veatch, E. T. Fossel and E. R. Blout, *Biochemistry*, 1974, **13**, 5249-5256.
24. D. A. Langa, *Science*, 1988, **241**, 188-191.
25. D. A. Kelkar and A. Chattopadhyay, *Biochimica et Biophysica Acta (BBA)-Biomembranes*, 2007, **1768**, 2011-2025.
26. A. M. O'Connell, R. E. Koeppe and O. S. Andersen, *Science*, 1990, **250**, 1256-1259.
27. E. Bamberg, H. Apell and H. Alpes, *Proceedings of the National Academy of Sciences*, 1977, **74**, 2402-2406.
28. O. Andersen, *Biophysical journal*, 1983, **41**, 119-133.
29. V. B. Myers and D. Haydon, *Biochimica et Biophysica Acta (BBA)-Biomembranes*, 1972, **274**, 313-322.
30. P. Mueller and D. Rudin, *Nature*, 1967, **213**, 603.